Plasmodium falciparum mitochondrial complex III, the target of atovaquone, is essential for progression to the transmissible sexual stages.

Pradeep Sheokand[1], Alexander Mühleip[1], and Lilach Sheiner[1*]

[1] Wellcome Centre for Integrative Parasitology, School of Infection and Immunity, University of Glasgow, Glasgow G12 8TA, UK

*Corresponding author: lilach.sheiner@glasgow.ac.uk

Abstract

The *Plasmodium* mitochondrial electron transport chain (mETC) is responsible for essential metabolic pathways such as *de novo* pyrimidine synthesis and ATP synthesis. The mETC complex III (cytochrome *bc1* complex) is responsible for transferring electrons from ubiquinol to cytochrome *c* and generating a proton gradient across the inner mitochondrial membrane, which is necessary for the function of ATP synthase. Recent studies revealed that the composition of *Plasmodium* complex III is divergent from humans, highlighting its suitability as a target for specific inhibition. Indeed, complex III is the target of the clinically used anti-malarial atovaquone and of several inhibitors undergoing pre-clinical trials, yet its role in parasite biology have not been thoroughly studied. We provide evidence that the universally conserved subunit, PfRieske, and the new parasite subunit, PfC3AP2, are part of *Plasmodium falciparum* complex III (PfCIII), with the latter providing support for the prediction of its divergent composition. Using inducible depletion, we show that PfRieske, and therefore PfCIII as a whole, is essential for asexual blood stage parasite survival, in line with previous observations. We further found that PfCIII is essential for gametocyte maturation. These phenotypes are linked to defects in mitochondrial functions upon PfRieske depletion, including increased sensitivity to mETC inhibitors in asexual stages and decreased cristae abundance alongside abnormal mitochondrial morphology in gametocytes. This is the first study which explores the direct role of the PfCIII in gametogenesis via genetic disruption, paving the way for a better understanding of the role of mETC in the complex life cycle of these important parasites and providing further support for the focus of antimalarial drug development on this pathway.

Introduction

Malaria is a deadly disease which causes significant morbidity and mortality around the globe. with 249 million cases and ~608,000 deaths reported in 2022 alone[1]. It is caused by mosquito-transmitted parasites of the *Plasmodium* spp. with *Plasmodium falciparum* being responsible for most fatal cases in human. The parasites have a complex life cycle with several life stages parasitising different tissues in the host and in the vector [2]. In the blood of the host the parasite life stages can be divided to the asexual stages, responsible for the disease symptoms, and the sexual, gametocyte, stages which can be taken up by mosquito during a bloodmeal thus initiating transmission. Drugs targeting both these stages exist and are use as one of the strategies for malaria control [3, 4]. The rapid emergence of drug resistance however threatens the current first-line therapies and highlights a need to develop new compounds [5]. A better understanding of pathways that are known to be drug targets may contribute to this goal.

One of these pathways is the *Plasmodium* mitochondrial electron transport chain (mETC). This pathway harnesses electrons from different metabolic pathways via a series of dehydrogenases, including malate quinone oxidoreductase (MQO), dihydroorotate dehydrogenase (DHODH), succinate dehydrogenase (complex II) and a type II NADH dehydrogenase (NDH2). The electrons are transferred between complexes of the mETC via the mobile carriers ubiquinone, which transfers electrons to complex III (also known as the cytochrome *bc1* complex), and cytochrome *c*, which transfers them to complex IV. At complex IV these electrons reduce oxygen to water. The main function of mETC mediated electron transfer in asexual parasites is the electrons harnessing necessary for the pyrimidine synthesis pathway [6]. Additionally, the movement of the electrons through the mETC complexes III and IV is coupled to the pumping of protons which generates a proton gradient across the inner mitochondrial membrane. The proton gradient is utilised by ATP synthase (complex V) to generate ATP. This process is collectively named oxidative phosphorylation (OXPHOS). While not essential for asexual blood stages (which generate most of its ATP via cytoplasmic glycolysis) ATP synthase becomes essential at the mosquito stage [7]. Therefore, the role of mETC, is essential in both critical stages of the parasite life cycle.

The *Plasmodium falciparum* mETC complex III (PfCIII) is a well-established drug target for the clinically used drug, Atovaquone (ATQ) [8-10] and for inhibitors undergoing pre-clinical trials such as the series of endochin-like quinolones (ELQs) [11-13]. In mammalians three subunits compose the catalytic core of complex III: 1) the mitochondrially encoded cytochrome b (cytb), which spans the inner mitochondrial membrane and thus connects the two substrate binding sites named Qo and Qi; 2) cytochrome c1 (cytC1) and 3) Rieske. The last two together mediate the transfer of electrons between the two mobile carriers. The human complex III consists of eight further non-catalytic subunits [14]. PfCIII is proposed to consist of 12 subunits, which include homologs of cytb, cytC1 and Rieske, but not all eight non-catalytic subunits found in human have homologs [15]. Moreover, additional three apicomplexan specific subunits (PfC3AP1, PfC3AP2, PfC3AP3) are proposed to be part of PfCIII [15]. Despite its divergence and importance as a drug target, the composition and function of PfCIII is not fully understood.

In this study we provide support for the previously proposed divergent PfCIII composition through co-immunoprecipitation, localization, and gel migration of endogenously tagged proteins, while focusing on one conserved (PfRieske) and one apicomplexan unique (PfC3AP2) subunits. Using conditional

knockdown, we demonstrate that PfRieske is required for PfCIII function, and confirm that the complex is required for asexual blood stage survival whereby PfRieske depleted parasites show a defect in pyrimidine synthesis and become hypersensitive to mETC inhibitors, in line with previous reports of PfCIII disruption [10, 16]. We further found that PfRieske depletion resulted in a defect in gametocyte stage progression which coincide with a defect in mitochondrial cristae formation. This work provide support to the predicted role of PfCIII in the mitochondria of asexual and sexual *Plasmodium* stages and highlight the pathways it contributes to.

Results

PfRieske and PfC3AP2 are part of Plasmodium falciparum complex III (PfCIII)

Recent studies of the apicomplexan mETC complex composition via complexome profiling in both *Plasmodium falciparum* and *Toxoplasma gondii* have shown that their complex III consist of 12 and 11 subunits respectively [15, 17]. Both studies further identified new proteins that have no clear homologs in the mammalian complex [15, 17]. In *Plasmodium* three new proteins (PfC3AP1, PfC3AP2, PfC3AP3) are annotated as putative PfCIII subunits. To provide support for this divergent subunit composition we created tagged lines of two subunits, the parasite specific PfC3AP2 and the conserved PfRieske. While engineering the tagged lines we already included also the glmS system for inducible gene depletion [18]. Thus, we generated PfC3AP2-HA-glms and PfRieske-HA-glmS transgenic parasite lines whereby the c-terminal of each gene is fused with the HA-glmS tag, and the fusion proteins are expressed under the native promoter of the respective genes (Figure 1A). The correct integrations of the HA-glmS tags in the target loci was confirmed by PCR analysis (Figure 1B) and by western blot analysis (Figure 1C). Native migration and western blot analysis, used previously to resolve mETC complexes in the related apicomplexan *T. gondii* [17], further showed that both the proteins migrated at the same size of ~730 kDa (Figure 1D) in line with the predicted size of a PfCIII dimer based on its proposed composition [15]. This provided validation that both proteins are part of the complex. Further, we performed immunoprecipitation under native conditions with the PfRieske-HA-glmS transgenic parasite line (Figure 1E) followed by mass spectrometry analysis (Table S1). We found nine of the expected twelve subunits (Table 1) including PfC3AP2, providing support for the proposed composition and further validating that both subunits are part of PfCIII.

Expected	Detected	Mass (Da)	Accession
Cytb	Yes	43747	PF3D7_MITO2300
Cytc1	Yes	46613	PF3D7_1462700
Rieske	Yes	41354	PF3D7_1439400
QCR6	Yes	1100	PF3D7_1426900
QCR7	Yes	23119	PF3D7_1012300
QCR8	No	17000	PF3D7_0306000
QCR9	No	11700	PF3D7_0306000
MPPalpha	Yes	56440	PF3D7_0622600
MPPbeta	Yes	62189	PF3D7_0523100
C3AP1	No	9500	PF3D7_0722700
C3AP2	Yes	19557	PF3D7_1326000
C3AP3	Yes	6200	PF3D7_0817800

Table 1. The interacting partners of the *Pf*Rieske identified via immunoprecipitation and mass spectrometry analysis. Full MS data in Table S1.

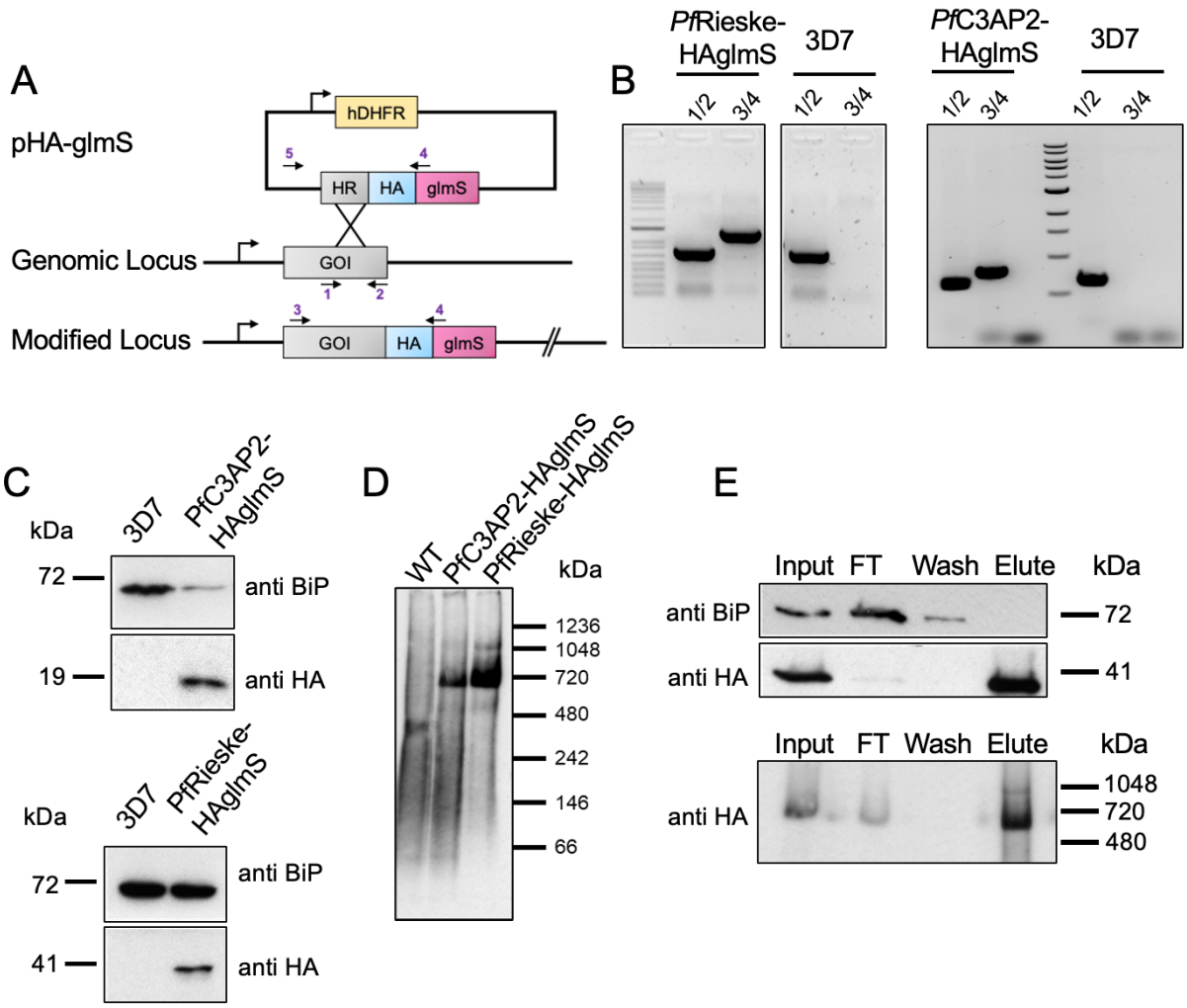

Figure 1. Tagging analysis and Immunoprecipitation of the PfRieske and PfC3AP2: (A) Schematics of the endogenously C terminal tagging strategy. **(B)** PCR analysis confirming the regulatable cassette integration using primers corresponding to the scheme in (A). **(C)** SDS-PAGE western blot of endogenously tagged *Pf*Rieske and *Pf*C3AP2 using anti HA antibody and anti BiP as a loading control. **(D)** BN-PAGE western blot of both tagged proteins using anti HA antibody. **(E)** Denaturing (top panels) and native (bottom panel) PAGE and western blots of immunoprecipitation fractions from PfRieske-HA-glmS line, showing the HA enrichments and the high migrating complex found in the elute. Anti-Bip antibodies were used as fraction specificity control.

Next, we used the endogenous tags to analyse the localisation of both proteins using anti HA antibody via immunofluorescence. We observed the signal in both asexual blood stages as well as gametocytes stages of the parasite. The signal could not be detected in asexual ring stages, potentially due to their small size causing a detection issue, but manifested as a tubular shape in trophozoites and became branched in the schizonts (Figure 2A, Figure 3A). In gametocytes the signal is seen to be in elongated tubular like structure (Figure 2B, Figure 3B). These observations are in line with a mitochondria shape [19, 20]. In agreement with this, both the proteins co-localise with MitoTracker-Red which confirms the predicted localisation of these proteins to the mitochondria (Figure 2C-D. Figure 3C-D). Western blot analysis confirmed the expression of both proteins across the different stages of the asexual blood cycle (Figure 2E, Figure 3E).

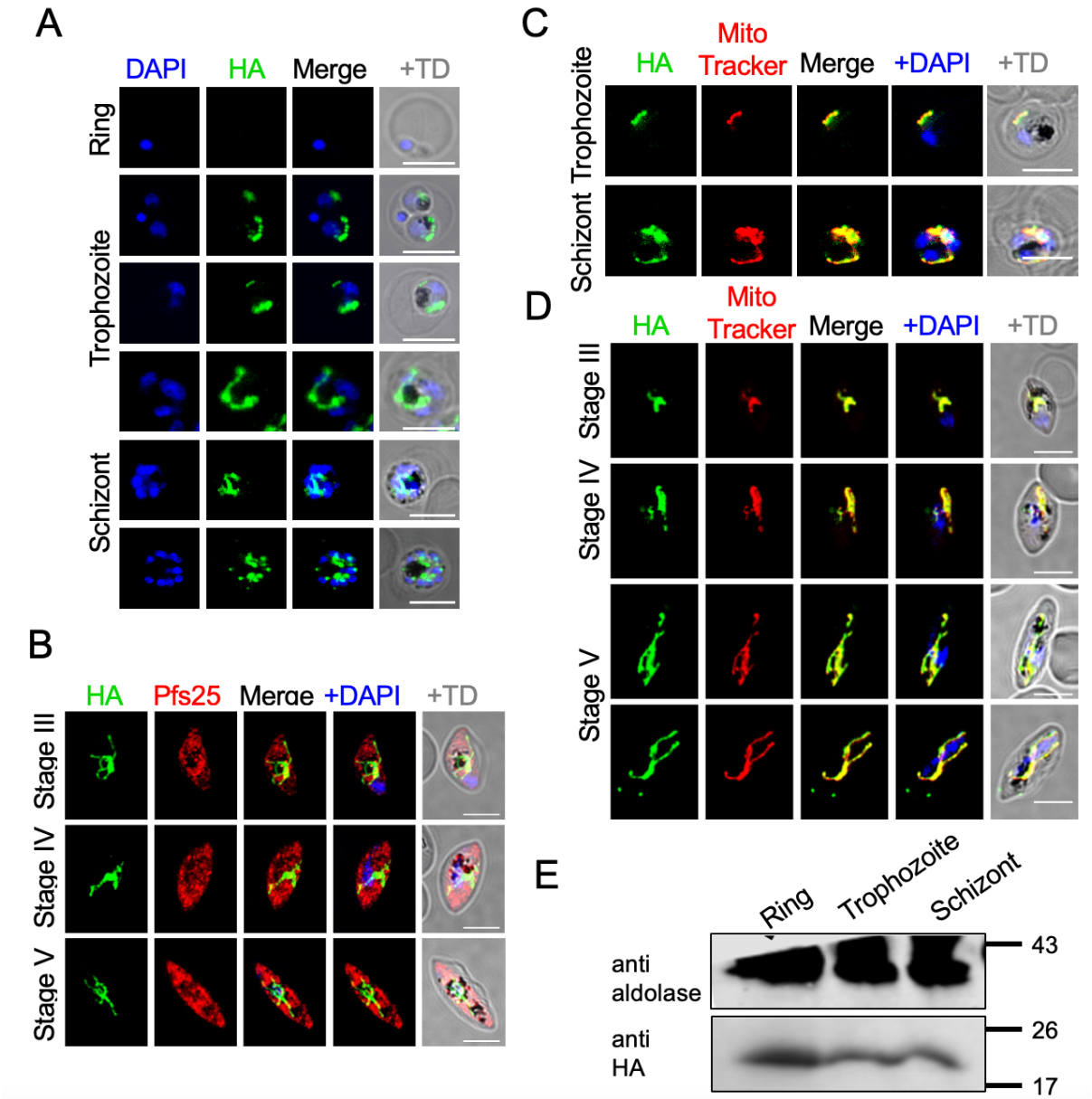

Figure 2. Expression and subcellular localisation of PfRieske in P. *falciparum*. (A,B) Immunofluorescence assay of PfRieske, visualised with anti-HA, in asexual blood stages (A) and in gametocytes (B). **(C,D)** Immunofluorescence assay of PfRieske visualised with anti-HA and co-stained with MitoTracker-Red showing colocalization in both asexual (C) and sexual (D) blood stage parasites. Scale bar: 5µm. **(E)** Western blot showing the expression of the PfRieske across the different developmental stages of the asexual blood stage cycle. The membranes were probed with anti- HA antibody and anti-aldolase was used as a loading control.

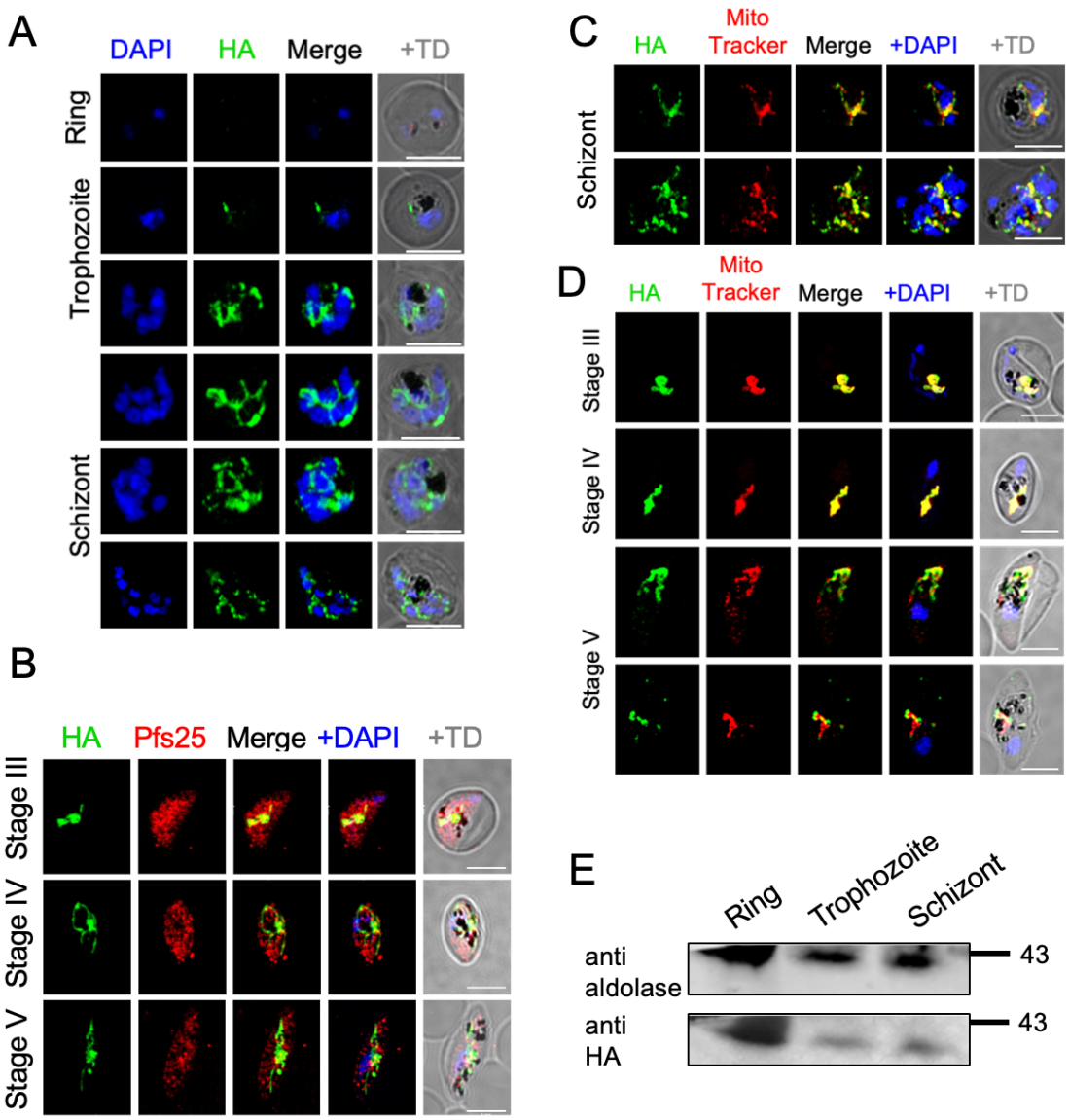

Figure 3. Expression and subcellular localisation of PfC3AP2 in P. *falciparum*. (A,B) Immunofluorescence assay of PfC3AP2, visualised with anti-HA, in asexual blood stage (A) and in gametocytes (B). **(C,D)** Immunofluorescence assay of PfC3AP2 visualised with anti-HA and co-stained with MitoTracker-Red showing colocalisation in both asexual (C) and sexual (D) blood stage parasites. Scale bar: 5µm. **(E)** Western blot showing the expression of the PfC3AP2 across the different developmental stages of the asexual blood stage cycle. The membranes were probed with anti- HA antibody and anti-aldolase was used as a loading control.

PfRieske is essential for parasite growth.

The importance of PfCIII for *Plasmodium* survival is well established both based on numerous inhibitor sensitivity and resistance mutant analyses [21-25], and, more recently, through the study of the subunit cytC1 [16]. However, the impact of PfCIII disruption on parasite biology has not been fully characterise. To address this gap, we focused on the two subunits we validated here and attempted their genetic disruption. We used the HA-glmS lines to induce a knockdown of each gene. Western blot analyses using the HA tag showed a significant decrease in the levels of both PfC3AP2 and PfRieske when parasites were grown in the presence glucosamine (GlcN) (Figure 4A,B). To address the effect of these knockdowns on parasite growth, we cultured the PfRieske-HA-glmS and PfC3AP2-HA-glmS parasites in presence of the GlcN (from here on this condition is named Rieske-iKD and C3AP2-iKD respectively) and monitored the growth over four and eight 48h-long intra-erythrocytic cycles (IDCs) respectively. We did not observe a growth defect in C3AP2-iKD even after seven IDCs (Figure 4A). On the other hand, a severe growth defect at three IDC was seen upon PfRieske depletion (Rieske-iKD) (Figure 4B). Giemsa stained Rieske-iKD parasites seem morphologically similar to their parental control for two IDCs and the growth defect was observed at the late-trophozoite-to-early-schizont stage in the third IDC which is confirmed by stage quantification analysis of the Rieske-iKD parasites compared with the parental control (Figure 4C-F). These data indicate that the PfRieske subunit is essential for asexual parasites development.

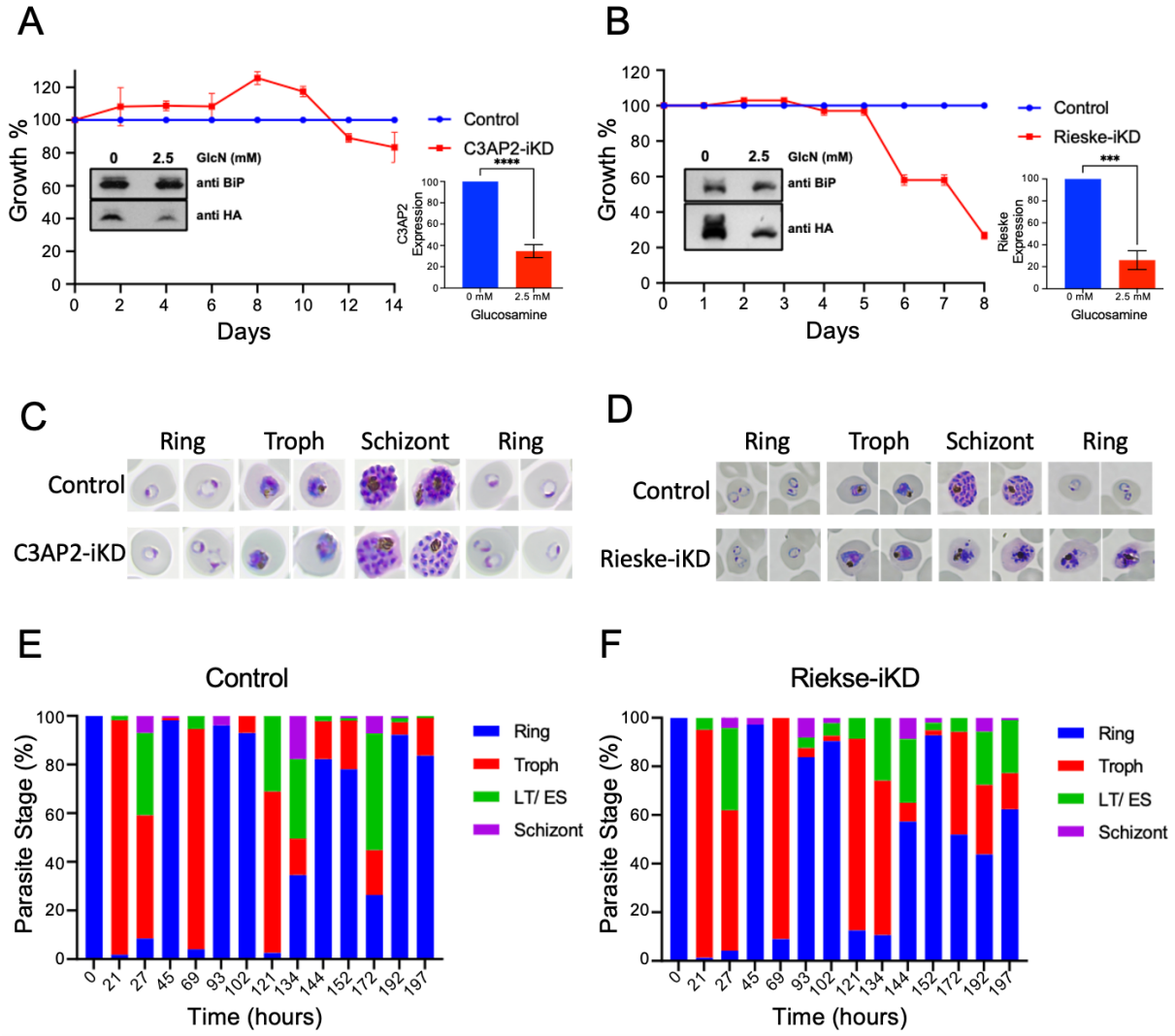

Figure 4. Inducible knockdown shows that PfRieske is essential for the asexual blood stage parasite growth: (A,B) Growth curves of C3AP2-iKD n = 2 (A) and Rieske-iKD n = 3 (B) transgenic parasites growing in presence and absence of the 2.5 mM glucosamine (GlcN). Insets are showing western blots probed with anti-HA and anti-Bip antibodies of the parasite cell lysate grown in GlcN presence and absence condition. Error bars are SEM. **(C,D)** Representative images of Giemsa-stained smears of the third cycle of the C3AP2-iKD (C) and Rieske-iKD (D) parasites grown in presence or absence of GlcN. **(E,F)** Bar graph showing quantification of the life stage progression of the Rieske-iKD parasites in absence (E) and presence (F) of GlcN n = 2 for both.

Loss of PfRieske results in hypersensitivity to mETC inhibitors and to membrane depolarisation by proguanil.

Several compounds are well-established inhibitors of enzymes involved in the transport of electrons in the *Plasmodium* mitochondrion. PfCIII is known to be inhibited by atovaquone [8-10]; DHODH is targeted by DSM-265 [26]; and, while the direct target of proguanil is not fully resolved, it is believed to disrupt the mitochondrial membrane potential too [6, 27]. Parasites with decreased expression of the targets of those compounds are expected to be hypersensitivity to their inhibition. This was demonstrated in a study of the *Plasmodium* mitochondrial ribosome (mitoribosome). Disruption of the mitoribosome leads to a decrease in functional PfCIII because one of the PfCIII components, cytb, is encoded in the mitochondrial genome, and indeed such disruption led to hypersensitivity to atovaquone, DSM-265 and proguanil [28]. Likewise, as we suspect that PfRieske depletion in our line results in decrease of functional PfCIII, we hypothesised that it would lead to similar hypersensitivity. Seeing that the growth defect following PfRieske depletion is detected on day six (third IDC), we added inhibitors on day four (at the ring stage of the second IDC) and monitored the parasite growth over the next cycle, IC_{50} were then calculated on day six (Figure 5A). In line with our hypothesis, Rieske-iKD parasites show hypersensitivity towards atovaquone, DSM-265, and proguanil (Figure 5B). The IC_{50} for chloroquine and artemisinin, which do not interfere with the mETC, remained unchanged compared to wild type (Figure 5C), indicating that the observed hypersensitivity is specific to inhibition of this pathway.

Since electron transport is coupled to proton pumping, which in *Plasmodium* is expected to occur in Complexes III and IV, we reasoned that PfRieske depletion will reduce the mitochondrial membrane potential. We used MitoTracker-Red as a proxy for membrane potential and investigated the effect of PfRieske depletion and mETC inhibitors on its signal distribution. Rieske-iKD parasites grown in presence of GlcN for five days still presented MitoTracker-Red mitochondrial specific staining, as did parasites treated with atovaquone (1 nM) or proguanil (1 µM) alone (Figure 5D). However, parasites treated with both atovaquone and proguanil loss the membrane potential dependent mitochondrial staining of MitoTracker-Red and the signal was detected in the cytosol instead (Figure 5E). Likewise, treatment of PfRieske-HA-glmS with both GlcN and proguanil resulted in loss of the mitochondrial staining (Figure 5E). These data indicate that the depletion of PfRieske disrupts the membrane potential in a manner that mimics the disruption caused by inhibition with 1 nM of atovaquone.

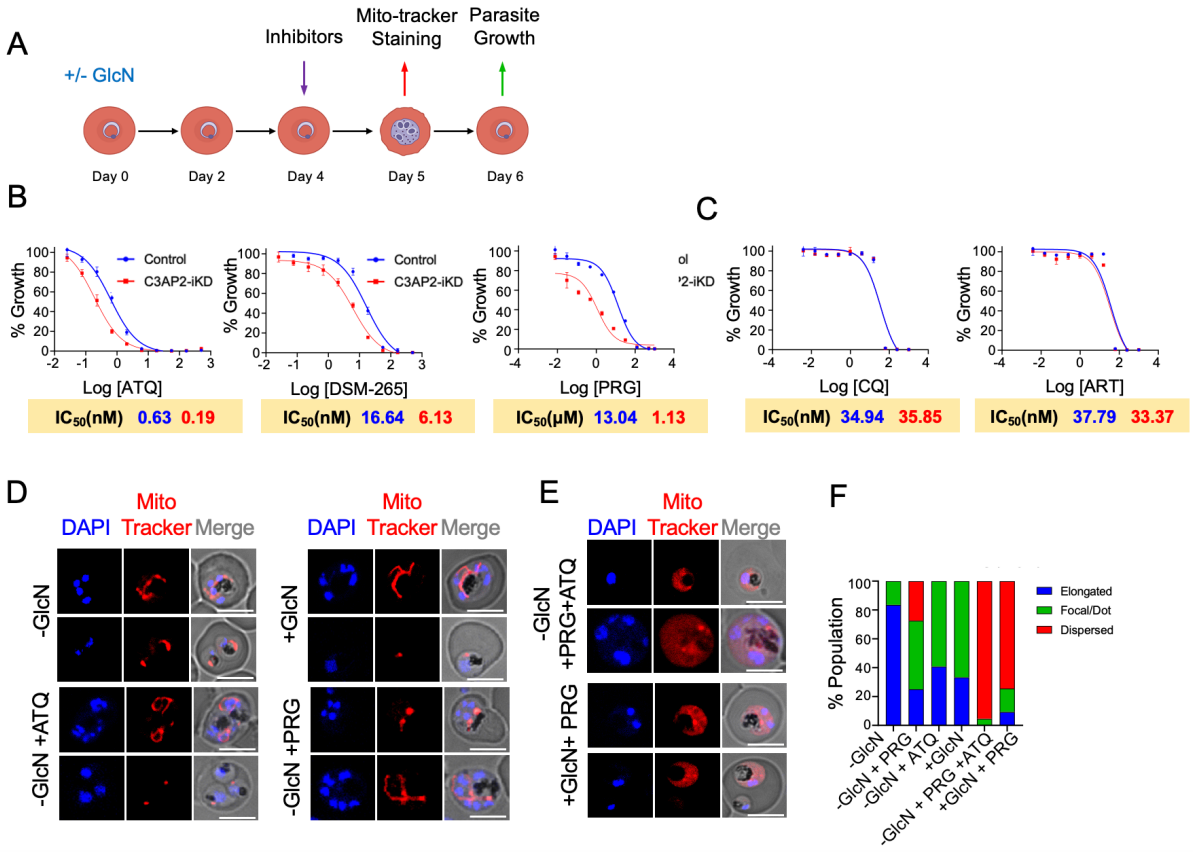

Figure 5. Depletion of PfRieske results in mETC failure: (A) Schematic representation of our experimental setup for the membrane potential and hypersensitivity assays. **(B)** IC_{50} analysis reveals hypersensitivity of GlcN treated parasites (Rieske-iKD) to the mETC inhibitors atovaquone (ATQ), DSM-265 and proguanil (PRG). **(C)** IC_{50} analysis confirms no change in the sensitivity of GlcN treated parasites (Rieske-iKD) to drugs used as negative control for (B), Chloroquine (CQ) and Artemisinin (ART). The graphs in B and C are each a representative from n=3 independent experiments, and the numbers are the mean of the triplicates. **(D,E)** confocal fluorescent microscopy images of MitoTracker-Red stained parasites grown in the presence or absence of glucosamine, atovaquone and proguanil (-/+ GlcN/ ATQ / PRG). Combinations that do not affect the membrane potential are shown in (D) as controls, while treatment with atovaquone and proguanil, or upon PfRieske depletion and proguanil treatment are shown in (E). Scale bar: 5μm **(F)** Quantification of the mitochondrial signal in each of the conditions in (D) and (E). The data shown is representative of the n=2 independent experiments.

PfRieske is required for the pyrimidine synthesis pathway.

The profile of hypersensitivity to inhibitors and the observed disruption of the mitochondrial membrane potential upon PfRieske depletion is in line with a decrease in functional PfCIII in this mutant. Previous studies demonstrated that the main function of PfCIII in asexual stage parasites is in ubiquinone recycling for the DHODH-ubiquinone oxidoreduction cycle which is an essential step in the pyrimidine synthesis pathway [6]. We thus hypothesised that the observed growth defect is due to a defect in the pyrimidine synthesis pathway. Since we observed the growth arrest in the third cycle (Figure 4B) we isolated whole-cell metabolites from the trophozoite stage of this cycle (on day five) and performed targeted metabolomic analysis for intermediates of the pyrimidine synthesis pathway

that are found upstream of DHODH: *N*-carbamoyl-L-aspartate and dihydroorotate (Figure 6A). We found that the level of both metabolites was significantly enhanced (~4 folds increase) in the Rieske-iKD (Figure 6B), suggesting that they accumulate in this mutant. As a positive control we analysed those metabolites in parasites that were treated with 10 nM atovaquone for four hours which also resulted in the accumulation of these metabolites as expected (Figure 6B).

Previous studies have demonstrated that the need for PfCIII to oxidize ubiquinol to ubiquinone for the cycle of DHODH-ubiquinone oxidoreduction can be bypassed through addition of the ubiquinone analogue decyl-ubiquinone (dQ) to the parasite growth media [16, 29, 30]. It would therefore be expected that the observed growth defect upon PfRieske depletion should be rescued with dQ. Accordingly, parasites grown in the presence of both GlcN and dQ showed restored growth comparable to parasites grown in the absence of GlcN (Figure 6C). Taken together these data provide additional support that PfRieske is required for PfCIII function and suggests that the observed growth defect of asexual stages in our mutant is likely due to a defect in pyrimidine synthesis.

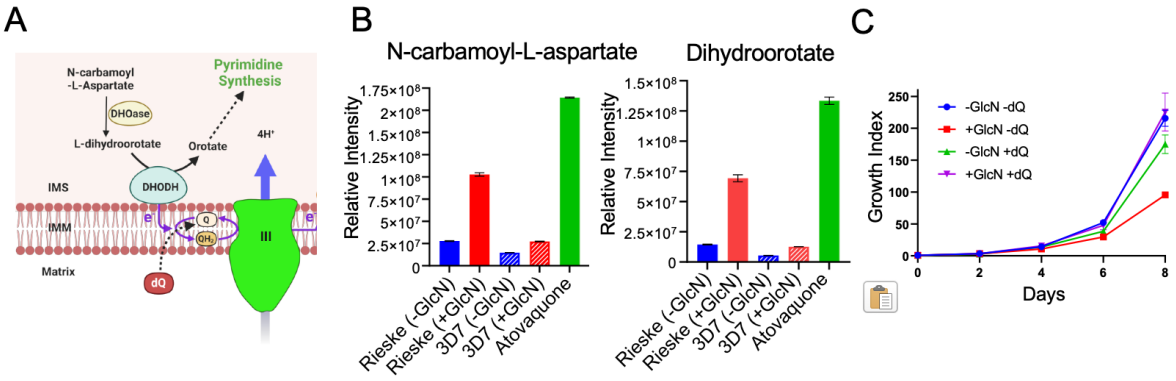

Figure 6. Accumulation of pyrimidine synthesis precursors in Rieske-iKD, while treatment with decyl-ubiquinone rescues its growth defect: (A) schematic image of the part of the pyrimidine synthesis pathways involving DHODH, ubiquinone and PfCIII. The mitochondrial intermembrane space (IMS), inner membrane (IMM), Ubiquinol (QH_2), ubiquinone (Q) and decyl-ubiquinone (dQ) are shown. **(B)** Bar graph showing the levels of the analysed pyrimidine synthesis pathway intermediates, N-cabamoyl-L-aspartate (left) and Dihydroorotate (right), in parental and Rieske-iKD lines grown in the presence or absence of GlcN (Rieske / 3D7 (-/+ GlcN) or upon treatment with atovaquone. **(C)** Growth curve of Rieske-iKD in presence and absence of GlcN (-/+ GlcN) and of 30 µM dQ (-/+ dQ). Errors bars are SEM.

Loss of PfRieske causes decrease in cristae density and affects gametocytes maturation.

The transition from asexual stages to gametocyte is accompanied by a shift in carbon metabolism whereby gametocytes rely more on the TCA cycle, mETC and ATP synthase for energy and metabolites [31, 32]. In line with this shift, mETC components show up to 40-fold increase in expression in the sexual stages [15]. We therefore expect that PfCIII will play a critical role in more pathways in gametocyte biology compared to the asexual stages. This is supported by the finding that

285 development and transmission in mosquitos depends on a fully functional PfCIII [21, 33, 34]. We were
286 therefore interested to examine the impact of PfRieske depletion on gametocytes development. We
287 induced gametocyte commitment using the spent-medium protocol [35] (Figure 7A,B). Morphological
288 analysis revealed that gametocyte development was severely affected upon PfRieske depletion: in the
289 control set, 100 % of the parasites analysed reach stages IV/V, whereas ~30% abnormal gametocytes
290 were seen in Rieske-iKD (Figure 7B,C). Abnormal gametocytes were characterised with round overall
291 morphology and what seem to be a swollen food vacuole (Figure 7B,D).
292
293 Mitochondrial cristae shape is tightly linked to oxidative phosphorylation (OXPHOS) activity.
294 Accordingly, the metabolic shift in gametocytes coincides with *de novo* appearance of cristae [7, 36,
295 37]. We thus hypothesised that the defect in gametocyte development upon PfRieske depletion would
296 be linked to cristae abnormalities. In support of this hypothesis, examination of the Rieske-iKD
297 parasites using transmission EM (TEM) revealed abnormal mitochondrial morphology upon PfRieske
298 depletion (Figure 7D). Quantification of cristae numbers per mitochondrial area further showed that
299 these parasites have a reduced cristae density in their mitochondria compared with their parental line
300 (Figure 7E). To our knowledge this is the first time that a cristae defect is observed upon disruption of
301 a *Plasmodium* gene. These data show that PfRieske is required for maintaining the cristae density in
302 *P. falciparum* gametocytes which may ultimately help the parasite in fulfilling the metabolic needs
303 required for gametocyte maturation.
304

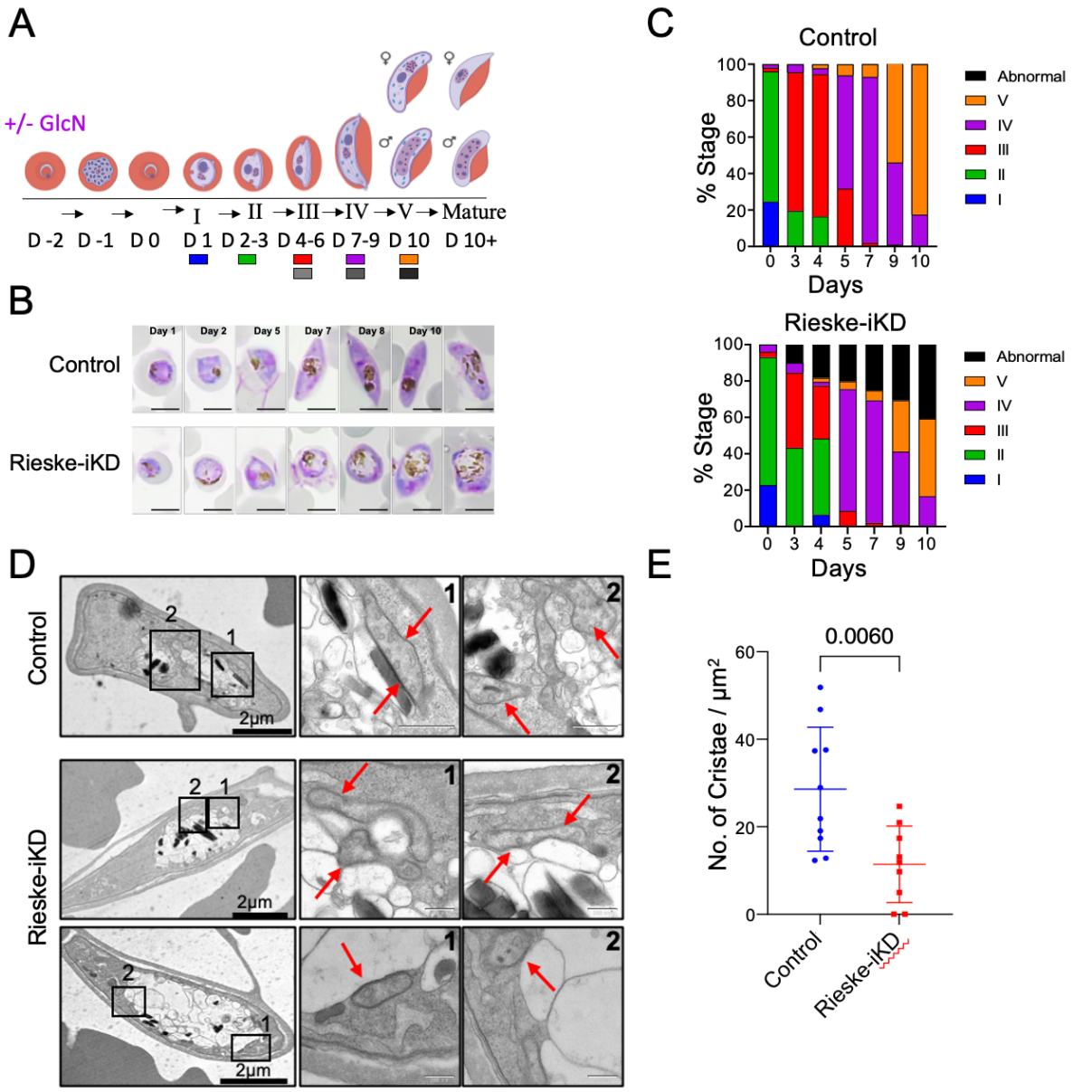

Figure 7. Knockdown of PfRieske arrests gametocyte development: (A) Schematics of the experimental setup of gametocyte induction in control and Rieske-iKD along with a scheme of the different stages. **(B)** Progression of the control and Rieske-iKD gametocytes monitored by giemsa stained smears. Scale bar: 5µm **(C)** quantification of morphologies based on giemsa-stained smears of control and Reiske-iKD gametocytes. **(D)** Transmission electron micrographs of the control and Rieske-iKD gametocytes. Enlarged sections show mitochondria (red arrows). Scale bar: 200nm **(E)** Quantification of cristae density in the control and Rieske-iKD gametocytes.

317 **Discussion**
318
319 The mETC is critical for the survival of many eukaryotic cells including both the apicomplexans and
320 their hosts, nevertheless the parasite pathway shows different sensitivity to inhibitors compared to
321 the human one. For this reason, the *Plasmodium* mETC has been the focus of numerous drug discovery
322 studies for antimalarial drug development, including a recent screen of the Medicines for Malaria
323 Venture (MMV) "pathogen box" [38]. Most of our knowledge about *Plasmodium* mETC complexes
324 including PfCIII is therefore based on studies using inhibitors or analysing drug-resistance, while their
325 role within parasite biology is less well understood. Here we use genetic disruption to provide
326 improved understanding of the role of PfCIII in parasite biology in asexual and sexual stages.
327
328 Recent studies in apicomplexans proposed a divergent set of mETC complex subunits compared to the
329 mETC of the host and highlighted new parasites subunits in each of the complexes [15, 17, 39, 40].
330 PfCIII was proposed to consist of 12 subunits with a predicted higher molecular size compared to
331 human complex III [15]. Via C-terminal tagging we provided support for this prediction by recovering
332 some of the new subunits in immunoprecipitation and via BN-PAGE and western analysis which
333 confirmed that both the conserved PfRieske and the new subunit PfC3AP2 are part of a complex which
334 migrates at size of ~730 kDa. It will be of interest to understand how the new subunit contribute to
335 PfCIII function and what is their mechanism of action in this important complex. One possibility is that
336 they would structurally "fill-in" for the missing homologs of the non-catalytic subunits found in other
337 systems, as we recently proposed for the non-catalytic subunits of mETC complex II in the related *T.*
338 *gondii parasite* [40]. Another option is that they may mediate interaction with other mETC complexes
339 to form supercomplexes, as suggested for non-catalytic and species-specific subunits in other systems
340 [41]. Importantly, regardless of their function, the presence of different proteins in PfCIII compared to
341 its human counterpart may well induce small changes in the location and orientation of amino acid in
342 and around the substrate binding pockets that could affect the interaction of PfCIII with inhibitors and
343 that may provide opportunities for new drug development. Structural analysis of PfCIII will likely help
344 shed light on these open questions.
345
346 Considering the essential role of PfCIII demonstrated in previous inhibitor studies, it is expected that
347 its subunits will be important for parasite survival. In agreement with this expectation a previous study
348 shows that a conditional depletion of mACP which leads to secondary loss of PfRieske ultimately leads
349 to asexual stage parasite death [30]. Likewise, depletion of cytC1 protein demonstrated its essentiality
350 for mETC functions and growth of asexual stages [16]. Our conditional knockdown adds support to
351 these observations by showing directly that PfRieske is essential for asexual growth. However, to our
352 surprise, PfC3AP2 protein downregulation did not have a significant impact on growth. This was
353 unexpected given that in the genome wide piggy bac transposons-based study *PfC3AP2* is predicted
354 to be essential for growth [42], and our previous study of the PfC3AP2 homolog from *T. gondii* also
355 showed that it is essential for parasite survival [17]. We cannot fully conclude weather the regulation
356 accomplished with the glmS system is not sufficiently tight or weather PfC3AP2 is truly dispensable
357 for asexual blood stage parasites at this point.
358
359 Previous studies demonstrated that disruption of a component of PfCIII [16] and of the *P. falciparum*
360 mitoribosome [43] (required to translate the essential PfCIII subunit cytb), leads to parasites
361 hypersensitive for mETC inhibitors, likely since there is less PfCIII activity remaining to inhibit in those

362 mutants. Studies further suggested that a potential alternate pathway to polarise the inner
363 mitochondria membrane independent of complex III and complex IV exists in *Plasmodium* [6, 44]. This
364 pathway can be blocked by proguanil only in the presence of a complex III inhibitor. We observed that
365 loss of PfRieske alone did not result in membrane depolarisation, which instead required a
366 combination of PfRieske depletion and treatment with proguanil. Collectively, our observations thus
367 agree with previous findings, thus providing support that PfRieske depletion results in PfCIII disruption
368 in our case too.
369
370 The mETC plays two major cellular functions: the one is the electron transfer, whereby the transported
371 electrons reduce a final electron acceptor, often oxygen. This electron transfer function enables
372 different metabolic pathways through oxidation of key enzymes, such as DOHOD of the pyrimidine
373 synthesis pathway; the other is oxidative phosphorylation, whereby the electrons transported from
374 TCA cycle metabolites are coupled to the pumping of protons by mETC complexes, generating an
375 electrochemical gradient that facilitates ATP synthesis by ATP synthase. The *P. falciparum* life cycle is
376 complex, consisting of multiple developmental stages and requiring survival in two hosts. The different
377 stages and the moves between host environments manifest in major metabolic shifts and the reliance
378 on different roles of the mETC is expected to vary accordingly. For example, it was established that in
379 the asexual blood stages the main function of *P. falciparum* mETC is enabling the oxidation of DHODH
380 for *de novo* pyrimidine synthesis [6]. Our metabolomic data confirms that PfRieske depletion results
381 in defect in the pyrimidine synthesis pathway and accumulation of two key metabolites downstream
382 of DHODH. Likewise, the ability of dQ to rescue the growth of PfRieske depleted parasites, which is in
383 line with previous observations [16, 29], provides further support for the sole role of ubiquinone
384 recycling that PfCIII plays in the asexual blood-stages.
385 On the other hand, different findings point to the importance of active oxidative phosphorylation in
386 the transmissible gametocyte stages, including the increased expression of genes encoding mETC
387 components in gametocyte [15], and the growth defect of different life stages upon disruption of other
388 mETC enzymes such as complex II, ATP synthase and NDH2 in *P. berghei* [7, 45, 46]. Likewise,
389 mitochondrial cristae, which are a hallmark of active oxidative phosphorylation are almost only
390 present in the sexual stage parasites among of the blood stage parasites. In line with these
391 observations, we found a defect in gametocyte development upon PfRieske depletion, and this
392 outcome coincides with reduced cristae density in those PfRieske depleted gametocytes. In another
393 protozoan, *Tetrahymena thermophila*, complex III is a part of a supercomplex that plays a role in
394 curving the cristae [47]. It is possible that one of the PfCIII containing supercomplexes that were
395 detected in *Plasmodium* and that were found to be more abundant in sexual compared with asexual
396 stages [15] plays a similar role in these parasites. In this scenario, PfCIII depletion would lead to a
397 decrease in the number of any supercomplexes involving it, and thus to the observed cristae formation
398 defect. However, the mechanism controlling cristae biogenesis in *P. falciparum* requires further
399 studies at this point. Interestingly, on top of the mitochondrial ultrastructure defect, PfRieske depleted
400 gametocytes also show an enlarged food vacuole. Seeing that the food vacuole plays a central role in
401 parasite metabolism via haemoglobin degradation and recycling of amino acids, we speculate that the
402 functions of these two organelles are tightly coordinated and that the two phenotypes are potentially
403 linked. The apicomplexan mitochondrion is seen to be involved in active membrane contact sites with
404 several organelles (ER, pellicles, nucleus [48-52]). It would be of interest to explore if there are
405 contacts with the food vacuole too.
406

Acknowledgements

We thank Dr. katarzyna modrzynska and Dr. Andrew Maclean for critical review of our manuscript. We acknowledge the support of Mathias Marti and his team with access to CAT3 facilities, and thank Gillian Parker for managing the facilities. We thank Leandro Lemgruber of the Glasgow Imaging Facility for his support and assistance in producing TEM data for this work. We thank Glasgow polyomics facility for their assistance in producing proteomics and metabolomics data for the work. We thank Prof. Paul Gilson (Burnet Institute) for sharing plasmids. The Wellcome Centre for Integrative Parasitology is supported by core funding from the Wellcome Trust [104111]. This work was further supported by Wellcome Investigator Award (217173_Z_19_Z) (to L. Sheiner);

Supplementary data

Table S1 – full list of the outcome from the proteomics analysis of PfRieske-HA immunoprecipitation. Subunits predicted to be part of PfCIII according to complexome studies and homology searchers are shown in yellow.

421 **Materials And methods**
422
423 **Plasmid construction, parasite culture, transfection, and transgenic line confirmation**
424 To generate the HA-glmS construct, C-terminal region of PfRieske and PfC3AP2 were PCR amplified
425 using primer sets (2448,2449 for C3AP2 and 2451, 2535 for Rieske) and cloned into HA-glmS vector in
426 *BglII* and *PstI* restriction sites. Plsamodium *falciparum* 3D7 strain was cultured under standard culture
427 conditions in RPMI media supplemented with 0.5% (W/V) Albumax (Invitrogen). To generate the HA-
428 glmS transgenic parasite lines, 3D7 parasites were synchronised repeatedly by sorbitol treatment and
429 100 ug of plasmid DNA for the respective gene was transfected in *P. falciparum* by electroporation
430 (0.310 kV and 950 µF) [53]. Transfected parasites were selected with WR 99210 (Jacobus
431 Pharmaceuticals). Clonal selection was done by serial dilution in 96 well plate and the integration were
432 confirmed by PCR using primer set (2718, 2797 for C3AP2 and 2719, 2797 for Rieske) and by western
433 blot analysis using anti HA antibody.

2448 PfC3AP2-FWD	GCAGATCTCCTTCAGATAGTAGGAAATTTG
2449 PfC3AP2-REV	GCCTGCAGC TGCGTGTTCAACTGA
2535 PfRieske-FWD-B	GCGGATCCCCTGTATTTCCAAGAAAACC
2451 PfRieske-REV	GCCTGCAGCTCCAATTTTTATCGTATTTTC
2718 PfC3AP2-Int1	CAAAAGAATTCAGGGTAAATTTATACCTTG
2719 PfRieske-Int1	GTATTCCTCCTGCATCTGAAGATC
2797 HAglmS-REV-1	TGATCTGCACACTCAGCCGGGA

434
435 **Inducible knockdown and parasite growth assay**
436 Both the transgenic parasite lines were tightly synchronized with repeated 5% sorbitol treatment. To
437 assess the knockdown at the protein level, 2.5mM glucosamine (GlcN) was added at the ring stage
438 and schizont stage parasites were harvested using saponin. The protein samples for western blotting
439 were prepared from these parasites. For the growth assay, parasites were cultured in with/ without
440 GlcN conditions for several cycles and the parasitaemia was assessed at different intervals by malaria
441 SYBR Green I- based fluorescence assay (MSF) using MACSQuant. Briefly, cells were incubated with
442 SYBR green for 20 minutes at 37 °C in dark followed by the 3 washings with 1 X PBS and these samples
443 were analysed MACSQuant system. For each set 100000 cells were counted to monitor the
444 parasitaemia. Uninfected RBCs were using as negative control. To assess the stage specific knockdown
445 effect, giemsa stained smears were prepared at different interval from the control and GlcN treated
446 parasites and analysed by light microscope. Thousand infected RBCs (iRBCs) were counted to check
447 the stage specific defect of the Rieske-iKD.
448
449 **Mitochondria enrichment and Immunoprecipitation**
450 Both the parasite lines (PfRieske-HA-glmS and PfC3AP2-HA-glmS) and the parent 3D7 parasites were
451 grown at large scale under standard cultured conditions. For each line, eight large dishes of 10% late
452 trophozoite-schizont stage parasites were harvested using the 0.15% saponin treatment. Parasites
453 pellets were washed with 1X PBS several times to remove the haemoglobin contamination. Enriched
454 mitochondrial fraction was purified from these parasites using the previous published protocols.
455 Briefly, saponin purified parasites cells were broken using the nitrogen cavitation at 1500 p.s.i. for 20
456 minutes and passed through the miltenyi Biotech MACS column to remove the hemozoin. This
457 material was further pelleted by centrifugation and used for further experiments.

458 **Immunoprecipitation and mass spectrometry**
459 The mitochondrial samples were resuspended into the lysis buffer (1 % DDM) and kept on rotor in
460 cold room for 2 hours for lysis. These were centrifuged at 16000 x g for 30 minutes and the supernatant
461 was used for the overnight binding on the Pierce anti-HA agarose beads. Next day, beads were washed
462 thrice with the lysis buffer and proteins were eluted by incubating the beads with HA peptide (1mg/ml)
463 overnight. Samples were collected at different steps and analysed by western blotting of both SDS-
464 PAGE and BN-PAGE. Beads and eluted samples were sent for mass spectrometry analysis.
465 For Mass spectrometry analysis trypsin digested peptide samples were prepared by using……. protocol
466 and these dry peptides residues were solubilized in 20 µL 5 % acetonitrile with 0.5 % formic acid using
467 the auto-sampler of a nanoflow uHPLC system (Thermo Scientific RSLCnano). Online detection of
468 peptide ions was by electrospray ionisation (ESI) mass spectrometry MS/MS with an Orbitrap Elite MS
469 (Thermo Scientific). Ionisation of LC eluent was performed by interfacing the Sharp Singularity
470 emitters (Fossil Ion Tech) with an electrospray voltage of 2.5 kV. An injection volume of 5 µL of the
471 reconstituted protein digest were desalted and concentrated for 1.1 min on trap column (0.3 × 5 mm)
472 using a flow rate of 25 µl / min with 1 % acetonitrile with 0.1 % formic acid. Peptide separation was
473 performed on a Pepmap C18 reversed phase column (50 cm × 75 µm, particle size 3 µm, pore size 100
474 Å, Thermo Scientific) using a solvent gradient at a fixed solvent flow rate of 0.3 µl / min for the
475 analytical column. The solvent composition was A) 0.1 % formic acid in water B) 0.08 % formic acid in
476 80% acetonitrile 20% water. The solvent gradient was 4 % B for 1.5 min, 4 to 60 % for 100.5 min, 60
477 to 99 % for 14 min, held at 99 % for 5 min. A further 9 minutes at initial conditions for column re-
478 equilibration was used before the next injection.
479 Protein identifications were assigned using the Mascot search engine (v2.6.2, Matrix Science) to
480 interrogate protein sequences in the *Plasmodium falciparum* 3D7 database. A mass tolerance of 10
481 ppm was allowed for the precursor and 0.3 Da for MS/MS matching.
482
483 **Denaturing polyacrylamide gel electrophoresis (SDS-PAGE), Blue native (BN-PAGE), and western**
484 **blotting**
485 For SDS-PAGE, Parasites were isolated by lysing the infected RBCs with 0.15% saponin and the
486 parasites were resuspended in Laemmli buffer and lysed by heating at 95 for 10 minutes. Proteins
487 were further separated on the 12% SDS-PAGE and transferred on the PVDF membrane (Millipore)
488 using semi dry trans-blot (Bio-Rad). For the BN-PAGE, samples were prepared by resuspended the
489 protein samples in solubilisation buffer and incubated on ice for 30 minutes and centrifuged at 16000
490 x g at 4C for 30 minutes. The supernatant was combined with sample buffer containing Coomassie
491 G250 (NativePAGE) at the final concentration of 0.25% DDM and 0.0625% Coomassie G250. The
492 samples were separated on the 4-16 % Bis-Tris native gel and transferred on PVDF membrane.
493 For the western blotting, membranes were incubated with blocking solution (5% skimmed milk in 1X
494 PBS) followed by overnight incubation with respective primary antibodies (anti HA rat 1:1000 (Roche),
495 anti BiP rabbit 1:5000 in cold room and 1 hr incubation with respective secondary antibodies (1:10000)
496 at room temperature and visualised by using ECL kit (Thermo-scientific).
497
498 **Immuno-fluorescence assay (IFA) and microscopy**
499 Infected RBCs (5-10% parasitaemia) were fixed in 4% paraformaldehyde and 0.05% glutaraldehyde for
500 50 min at room temperature on rotator. Cells were permeabilised by 10 minutes incubation with 0.1%
501 Triton X-100 on ice and incubated with blocking buffer (10% FBS in 1X PBS) for 90 minutes and then
502 probed with the primary antibody (anti-HA rat 1:100 (Roche) for 2 hours on rotor and after three

503 washing with 1x PBS cells were probed with anti-rat Alex Flour-488 (1:500) for 1 hour. Parasites nuclei
504 were stained with Hoechst with a final concentration of 5ug/ml. Images were captured by Nikon A1
505 confocal laser scanning microscope and analysed by Nikon-NIS element software (version 4.1). The 3D
506 images were constructed by using series of Z-stack images using IMARIS 7.0 (Bitplane Scientific)
507 software.
508 To label mitochondria infected RBCs were incubated with 100nM Mito Tracker Deep Red for 15
509 minutes at 37 ˚C shaker incubator and washed with 1x PBS thrice. Cells were further fixed and
510 processed for IFA as describes earlier.
511
512 **Metabolomic profiling**
513 Rieske-HAglmS parasites were synchronised, and knockdown assay was setup as describes earlier.
514 Parasites were isolated from the control and Rieske-iKD parasites using saponin and $3x10^8$ number of
515 parasites were used for metabolites isolation. Isolated parasites were quenched by rapidly cooling the
516 cells to 4 ˚C by dry ice/ethanol. Metabolites were isolated using chloroform/methanol/water (1:3:1)
517 method. Briefly, cells were resuspended in 600 µL of chloroform/methanol/water (1:3:1) and kept on
518 vortex for 1 hr at 4 ˚C. After centrifugation for 3 minutes at 13000 x g at 4 ˚C, supernatant was
519 transferred in to new eppendorf tube and stored in -80 ˚C until analysis by LC-MS.
520 Hydrophilic interaction liquid chromatography (HILIC) was carried out on a Dionex UltiMate 3000 RSLC
521 system (Thermo Fisher Scientific, Hemel Hempstead, UK) using a ZIC-pHILIC column (150 mm × 4.6
522 mm, 5 µm column, Merck Sequant). The injection volume was 10µl and samples were maintained at
523 5°C prior to injection. For the MS analysis, a Thermo Orbitrap QExactive (Thermo Fisher Scientific) was
524 used.
525 Metabolomics samples from the control samples (3D7 -/+ GlcN, 3D7 treated with ATQ) also prepared
526 and analysed in the same way.
527
528 **Drug sensitivity assay**
529 The drug assay was performed in 96 well plate. Rieske-HA parasites were grown in media with/without
530 GlcN for two cycles and second cycle ring parasites were exposed to drugs diluted in serial dilution. In
531 the third cycle parasites were lysed in SYBR green lysis buffer and fluorescence intensity was assayed
532 using spectrophotometer. IC_{50} graph for drugs were prepared using Graph prism software. All the
533 compounds used in this assay were purchased Atovoquone, DSM-265, Proguanil, Chloroquine,
534 Artemisinin
535
536 **Transmission electron microscopy**
537 For electron microscopy analysis, control and Rieske-iKD gametocytes were fixed with prewarmed 2%
538 glutaraldehyde in 0.1M cacodylate (pH 7.4) buffer. Following serial washes in 0.1M phosphate buffer,
539 samples were post-fixed in 1% OsO4 and 1.25% potassium ferrocyanide (vol:vol) in the same buffer
540 for 1 hour in the dark, washed with distilled water and contrasted EM bloc with 0.5% aqueous uranyl
541 acetate for 1 hour at room temperature in the dark. The samples were then dehydrated in acetone
542 ascending series (30%, 50%, 70%, 90%, 100%) and embedded in epoxy resin. Ultra-thin sections
543 (50nm) were sectioned in a Leica Ultramicrotome and collected in 100mesh grids covered with
544 formvar. The collected sections were contrasted with 2% aqueous uranyl acetate and later observed
545 in a Jeol 1200 transmission electron microscope (Jeol, Japan) operating at 80kV.
546
547 **Gametocyte commitment and culturing**

548 Gametocyte commitment assay was performed using well established protocol (>>>). Briefly, Rieske-
549 HA-glmS parasites were synchronised and divided in GlcN (+) or GlcN (-) conditions one cycle before
550 the commitment. Gametogenesis commitment was induced using nutritional stress by grown
551 parasites with spent medium (day two) and then growing parasites in media having heparin (1:500)
552 till day +three to block the invasion of the asexual stage parasites. After that parasites were cultured
553 with normal media conditions. Giemsa-stained smears were prepared at different time intervals for
554 the morphological analysis.
555
556

557 **References**

558 1. Organisation, G.W.H., *World Malaria Report 2022*. 2022.
559 2. Bray, R.S. and P.C. Garnham, *The life-cycle of primate malaria parasites.* Br Med Bull, 1982.
560 **38**(2): p. 117-22.
561 3. Delves, M., et al., *The activities of current antimalarial drugs on the life cycle stages of*
562 *Plasmodium: a comparative study with human and rodent parasites.* PLoS Med, 2012. **9**(2): p.
563 e1001169.
564 4. Cui, L., et al., *Antimalarial Drug Resistance: Literature Review and Activities and Findings of*
565 *the ICEMR Network.* Am J Trop Med Hyg, 2015. **93**(3 Suppl): p. 57-68.
566 5. Siqueira-Neto, J.L., et al., *Antimalarial drug discovery: progress and approaches.* Nat Rev Drug
567 Discov, 2023. **22**(10): p. 807-826.
568 6. Painter, H.J., et al., *Specific role of mitochondrial electron transport in blood-stage Plasmodium*
569 *falciparum.* Nature, 2007. **446**(7131): p. 88-91.
570 7. Sturm, A., et al., *Mitochondrial ATP synthase is dispensable in blood-stage Plasmodium*
571 *berghei rodent malaria but essential in the mosquito phase.* Proc Natl Acad Sci U S A, 2015.
572 **112**(33): p. 10216-23.
573 8. Fry, M. and M. Pudney, *Site of action of the antimalarial hydroxynaphthoquinone, 2-[trans-4-*
574 *(4'-chlorophenyl) cyclohexyl]-3-hydroxy-1,4-naphthoquinone (566C80).* Biochem Pharmacol,
575 1992. **43**(7): p. 1545-53.
576 9. Davies, C.S., et al., *The causal prophylactic activity of the novel hydroxynaphthoquinone*
577 *566C80 against Plasmodium berghei infections in rats.* Acta Leiden, 1989. **58**(2): p. 115-28.
578 10. Srivastava, I.K., H. Rottenberg, and A.B. Vaidya, *Atovaquone, a broad spectrum antiparasitic*
579 *drug, collapses mitochondrial membrane potential in a malarial parasite.* J Biol Chem, 1997.
580 **272**(7): p. 3961-6.
581 11. Winter, R.W., et al., *Antimalarial quinolones: synthesis, potency, and mechanistic studies.* Exp
582 Parasitol, 2008. **118**(4): p. 487-97.
583 12. Nilsen, A., et al., *Quinolone-3-diarylethers: a new class of antimalarial drug.* Sci Transl Med,
584 2013. **5**(177): p. 177ra37.
585 13. Winter, R., et al., *Optimization of endochin-like quinolones for antimalarial activity.* Exp
586 Parasitol, 2011. **127**(2): p. 545-51.
587 14. Guo, R., et al., *Architecture of Human Mitochondrial Respiratory Megacomplex I(2)III(2)IV(2).*
588 Cell, 2017. **170**(6): p. 1247-1257 e12.
589 15. Evers, F., et al., *Composition and stage dynamics of mitochondrial complexes in Plasmodium*
590 *falciparum.* Nat Commun, 2021. **12**(1): p. 3820.
591 16. Espino-Sanchez, T.J., et al., *Direct tests of cytochrome c and c(1) functions in the electron*
592 *transport chain of malaria parasites.* Proc Natl Acad Sci U S A, 2023. **120**(19): p. e2301047120.
593 17. Maclean, A.E., et al., *Complexome profile of Toxoplasma gondii mitochondria identifies*
594 *divergent subunits of respiratory chain complexes including new subunits of cytochrome bc1*
595 *complex.* PLoS Pathog, 2021. **17**(3): p. e1009301.
596 18. Sheokand, P.K., et al., *GlmS mediated knock-down of a phospholipase expedite alternate*
597 *pathway to generate phosphocholine required for phosphatidylcholine synthesis in*
598 *Plasmodium falciparum.* Biochem J, 2021. **478**(18): p. 3429-3444.
599 19. van Dooren, G.G., et al., *Development of the endoplasmic reticulum, mitochondrion and*
600 *apicoplast during the asexual life cycle of Plasmodium falciparum.* Mol Microbiol, 2005. **57**(2):
601 p. 405-19.
602 20. Okamoto, N., et al., *Apicoplast and mitochondrion in gametocytogenesis of Plasmodium*
603 *falciparum.* Eukaryot Cell, 2009. **8**(1): p. 128-32.
604 21. Goodman, C.D., et al., *Parasites resistant to the antimalarial atovaquone fail to transmit by*
605 *mosquitoes.* Science, 2016. **352**(6283): p. 349-53.
606 22. Komatsuya, K., et al., *Siccanin Is a Dual-Target Inhibitor of Plasmodium falciparum*
607 *Mitochondrial Complex II and Complex III.* Pharmaceuticals (Basel), 2022. **15**(7).

608 23. Xiang, H., et al., *Preclinical drug metabolism and pharmacokinetic evaluation of GW844520, a*
609 *novel anti-malarial mitochondrial electron transport inhibitor.* J Pharm Sci, 2006. **95**(12): p.
610 2657-72.
611 24. Yeates, C.L., et al., *Synthesis and structure-activity relationships of 4-pyridones as potential*
612 *antimalarials.* J Med Chem, 2008. **51**(9): p. 2845-52.
613 25. Winter, R.W., et al., *Evaluation and lead optimization of anti-malarial acridones.* Exp Parasitol,
614 2006. **114**(1): p. 47-56.
615 26. Coteron, J.M., et al., *Structure-guided lead optimization of triazolopyrimidine-ring substituents*
616 *identifies potent Plasmodium falciparum dihydroorotate dehydrogenase inhibitors with*
617 *clinical candidate potential.* J Med Chem, 2011. **54**(15): p. 5540-61.
618 27. Pudney, M., et al., *Atovaquone and proguanil hydrochloride: a review of nonclinical studies.* J
619 Travel Med, 1999. **6 Suppl 1**: p. S8-12.
620 28. Ling, L., et al., *Genetic ablation of the mitoribosome in the malaria parasite Plasmodium*
621 *falciparum sensitizes it to antimalarials that target mitochondrial functions.* J Biol Chem, 2020.
622 **295**(21): p. 7235-7248.
623 29. Ke, H., et al., *Variation among Plasmodium falciparum strains in their reliance on*
624 *mitochondrial electron transport chain function.* Eukaryot Cell, 2011. **10**(8): p. 1053-61.
625 30. Falekun, S., et al., *Divergent acyl carrier protein decouples mitochondrial Fe-S cluster*
626 *biogenesis from fatty acid synthesis in malaria parasites.* Elife, 2021. **10**.
627 31. MacRae, J.I., et al., *Mitochondrial metabolism of sexual and asexual blood stages of the*
628 *malaria parasite Plasmodium falciparum.* BMC Biol, 2013. **11**: p. 67.
629 32. Srivastava, A., et al., *Stage-Specific Changes in Plasmodium Metabolism Required for*
630 *Differentiation and Adaptation to Different Host and Vector Environments.* PLoS Pathog, 2016.
631 **12**(12): p. e1006094.
632 33. Paton, D.G., et al., *Exposing Anopheles mosquitoes to antimalarials blocks Plasmodium*
633 *parasite transmission.* Nature, 2019. **567**(7747): p. 239-243.
634 34. Paton, D.G., et al., *Using an antimalarial in mosquitoes overcomes Anopheles and Plasmodium*
635 *resistance to malaria control strategies.* PLoS Pathog, 2022. **18**(6): p. e1010609.
636 35. Saliba, K.S. and M. Jacobs-Lorena, *Production of Plasmodium falciparum gametocytes in vitro.*
637 Methods Mol Biol, 2013. **923**: p. 17-25.
638 36. Krungkrai, J., P. Prapunwattana, and S.R. Krungkrai, *Ultrastructure and function of*
639 *mitochondria in gametocytic stage of Plasmodium falciparum.* Parasite, 2000. **7**(1): p. 19-26.
640 37. Cogliati, S., J.A. Enriquez, and L. Scorrano, *Mitochondrial Cristae: Where Beauty Meets*
641 *Functionality.* Trends Biochem Sci, 2016. **41**(3): p. 261-273.
642 38. Hayward, J.A., et al., *A screen of drug-like molecules identifies chemically diverse electron*
643 *transport chain inhibitors in apicomplexan parasites.* PLoS Pathog, 2023. **19**(7): p. e1011517.
644 39. Seidi, A., et al., *Elucidating the mitochondrial proteome of Toxoplasma gondii reveals the*
645 *presence of a divergent cytochrome c oxidase.* Elife, 2018. **7**.
646 40. Silva, M.F., et al., *Functional and biochemical characterization of the Toxoplasma gondii*
647 *succinate dehydrogenase complex.* PLoS Pathog, 2023. **19**(12): p. e1011867.
648 41. Vercellino, I. and L.A. Sazanov, *Structure and assembly of the mammalian mitochondrial*
649 *supercomplex CIII(2)CIV.* Nature, 2021. **598**(7880): p. 364-367.
650 42. Zhang, M., et al., *Uncovering the essential genes of the human malaria parasite Plasmodium*
651 *falciparum by saturation mutagenesis.* Science, 2018. **360**(6388).
652 43. Dass, S., et al., *Transcriptional changes in Plasmodium falciparum upon conditional knock*
653 *down of mitochondrial ribosomal proteins RSM22 and L23.* PLoS One, 2022. **17**(10): p.
654 e0274993.
655 44. Skinner-Adams, T.S., et al., *Cyclization-blocked proguanil as a strategy to improve the*
656 *antimalarial activity of atovaquone.* Commun Biol, 2019. **2**: p. 166.
657 45. Hino, A., et al., *Critical roles of the mitochondrial complex II in oocyst formation of rodent*
658 *malaria parasite Plasmodium berghei.* J Biochem, 2012. **152**(3): p. 259-68.

659 46. Boysen, K.E. and K. Matuschewski, *Arrested oocyst maturation in Plasmodium parasites*
660 *lacking type II NADH:ubiquinone dehydrogenase.* J Biol Chem, 2011. **286**(37): p. 32661-71.
661 47. Muhleip, A., et al., *Structural basis of mitochondrial membrane bending by the I-II-III(2)-IV(2)*
662 *supercomplex.* Nature, 2023. **615**(7954): p. 934-938.
663 48. Mallo, N., et al., *Depletion of a Toxoplasma porin leads to defects in mitochondrial morphology*
664 *and contacts with the endoplasmic reticulum.* J Cell Sci, 2021. **134**(20).
665 49. Ovciarikova, J., et al., *Mitochondrial behaviour throughout the lytic cycle of Toxoplasma gondii.*
666 Sci Rep, 2017. **7**: p. 42746.
667 50. Oliveira Souza, R.O., et al., *IMC10 and LMF1 mediate mitochondrial morphology through*
668 *mitochondrion-pellicle contact sites in Toxoplasma gondii.* J Cell Sci, 2022. **135**(22).
669 51. Ovciarikova, J., et al., *Protein control of membrane and organelle dynamics: Insights from the*
670 *divergent eukaryote Toxoplasma gondii.* Curr Opin Cell Biol, 2022. **76**: p. 102085.
671 52. Connelly, S.V., et al., *Restructured Mitochondrial-Nuclear Interaction in Plasmodium*
672 *falciparum Dormancy and Persister Survival after Artemisinin Exposure.* mBio, 2021. **12**(3): p.
673 e0075321.
674 53. Crabb, B.S., et al., *Transfection of the human malaria parasite Plasmodium falciparum.*
675 Methods Mol Biol, 2004. **270**: p. 263-76.

676